

Special Article - Applications of Biosensors

Surface Plasmon Resonance Biosensors

Gorodkiewicz E^{1*} and Lukaszewski Z²

¹Department of Electrochemistry, University of Bialystok, Poland

²Faculty of Chemical Technology, Poznan University of Technology, Poland

*Corresponding author: Ewa Gorodkiewicz, Department of Electrochemistry, Institute of Chemistry, University of Bialystok, Ciolkowskiego 1K, 15-245 Bialystok, Poland

Received: July 06, 2019; Accepted: August 01, 2019;

Published: August 08, 2019

Abstract

A review is made of 86 papers on surface plasmon resonance biosensors, published between 2016 and mid-2019. The reviewed papers are categorized into four groups, depending on the degree of maturity of the reported solution: ranging from simple marker detection to a mature biosensor and analytical procedure. Instrumental solutions and details of biosensor construction are analyzed, including the chips, receptors and linkers used, as well as calibration strategies. Papers concerning the determination of micro RNA and large particles such as vesicles, exosomes and cancer cells are also reviewed. Biosensors with a sandwich structure containing different nanoparticles are considered separately, as are SPR applications for investigating the interactions of biomolecules. An analysis is also made of the markers determined using the biosensors. Concluding, there is shown to be a growing number of SPR applications in the solution of real clinical problems.

Keywords: Surface plasmon resonance; Cancer markers; Biosensors; Receptor immobilization; Antibodies; Nanoparticles

Introduction

Biosensors are the subject of enormous expectations and are gradually gaining in diagnostic importance. These expectations are connected with what is called 'liquid biopsy', i.e. diagnosis based on analysis of body fluids such as blood, urine and saliva, and the possibility of early diagnosis of various cancers or other diseases. However, there is still a shortage of biosensors offering near 100% sensitivity and specificity, i.e. respectively 100% of true positive and 0% of false positive results. An illustration of the relationship between true positive and false positive results is provided by ROC curves. An example of such curves obtained with the use of an SPRi biosensor for the determination of podoplanin in blood serum and urine is given in Figure 1. This example is evidence that SPR biosensors can be useful tools in the evaluation of the diagnostic efficiency of new biomarkers.

An ideal biosensor should react exclusively to the target marker despite the presence of numerous similar proteins, glycoproteins, etc. in the analyzed body fluid. Moreover, the biosensor's dynamic response range should include the concentrations of the marker found in the body fluid both of persons with the disease and of the healthy population. It is also expected that the precision of measurement of the marker concentration will be sufficient to distinguish between samples below and above a 'cut-off' value.

A limited number of measuring techniques are used successfully in combination with biosensors, the leader among which is ELISA. Surface Plasmon Resonance (SPR) is still only a promising technique. However, the number of applications of previously developed SPR biosensors in real clinical investigations is growing (Table 1).

This paper reviews the most recent publications on SPR biosensors, appearing between 2016 and early 2019, with a slight extension to include earlier papers by the authors. Earlier work is covered in excellent reviews by Masson [14] and Ferhan et al. [15]. Both Masson and Ferhan et al. conclude that future work should focus more on clinical samples than on improving detection specificity and

sensitivity.

Stages of biosensor development

Generally, a mature biosensor and a procedure for the determination of a particular marker are developed in several stages, beginning with the conception of the biosensor, followed by analytical characterization, validation, and determination of the marker in real samples. Therefore, the reviewed papers are categorized into four groups, depending on the degree of maturity of the reported solution. According to Gorodkiewicz and Lukaszewski [16], the following stages of development of a biosensor and a related analytical

Table 1: SPR biosensors applied in clinical investigations.

Disease	Marker	Reference
Bladder cancer	Podoplanin	[1]
Thermal injuries	20S proteasome	[2]
Bladder cancer	Cystatin C	[3]
Thermal injury	UCHL1	[4]
Burns	Laminin 5	[5]
Burns	Collagen IV	[5]
Burns	MMP2	[5]
Cryptorchidism	UCHL1	[6]
Acute Appendicitis	20S proteasome	[7]
Acute Appendicitis	UCHL1	[8]
Cryptorchidism	20S proteasome	[9]
Burns	20S Immunoproteasome	[10]
Appendicitis	Cathepsin B	[11]
Endometriosis	Cathepsin G	[12]
Endometriosis	Cathepsin G	[13]
Endometriosis	Cathepsin B	[13]
Endometriosis	Cathepsin D	[13]
Burns	20S Immunoproteasome	[67]

Table 2: Stages of biosensor development and technical solutions for biosensors used for the determination of cancer markers.

Stage	Marker	SPR type	Fluidic/ Non fluidic	Chip	Linker /receptor	Receptor immobilization	Reference
i	HER2	SPR	Micro-fluidic	Nano- whole array	Cysteamine/ Sandwich/ 2 Antibodies	Biotin/ streptavidin	[17]
i	CEA	SPR	Fluidic	Slide/Cr/Au	MUA /antibody	EDC/NHS	[18]
i	Cytokeratin 17	SPR	Non fluidic	Optical fiber/Au	S2PEG6COOH/ antibody	EDC/NHS	[19]
i	E-cadherin	SPR	nd	Au/mica	MUA/ antibody	EDC/NHS	[20]
i	CEA EGFR	SPR	nd	Grating/ Au/Al	nd	nd	[21]
ii	Cytokeratin-19	SPR	Both	Prism	Cysteamine/ GOCOOH/ /antibody	EDC/NHS	[22]
ii	PSA	SPR	Fluidic	Slide/Au/ MoS2QDs@g-C3N4@ CSAuNPs	PSA targeted aptamer	PSA targeted aptamer	[23]
ii	Cytokeratin 17	LSPR	Non-fluidic	Optical fiber Without Au	three protein A	1.covalent 2.electrostatic 3. protein A/antibody affinity	[24]
iii	PSA	SPRi	Fluidic	Slide/Au/	Allyl mercaptan	PSA imprinted polymer	[25]
iv	Rac1, Rac1b	SPR	Fluidic	CM5 chip	Dextran-COOH/ Antibody	EDC/NHS	[26]
iv	5LOX	SPR	Fluidic	CM5 chip	Dextran-COOH/ Antibody	EDC/NHS	[27]
iv	CDK4	SPR	Fluidic	CM5 chip	Dextran-COOH/ Antibody	EDC/NHS	[28]
iv	Laminin-5	SPRi	Non fluidic	Slide /Au/ Array	Cysteamine/ Antibody	EDC/NHS	[29]
iv	Collagen IV	SPRi	Non fluidic	Slide /Au/ Array	Cysteamine/ Antibody	EDC/NHS	[30]
iv	MMP1	SPRi	Non fluidic	Slide/Au/ Array	Cysteamine/ Antibody	EDC/NHS	[31]
iv	20S immune- proteasome	SPRi	Non fluidic	Slide /Au/ Array	1-octadecano-thiol / Inhibitor ONX 0914	Hydrophobic interaction	[32]
iv	MMP2	SPRi	Non fluidic	Slide /Au/ Array	1-octadecano-thiol / Inhibitor ARP 101	Hydrophobic interaction	[33]
iv	Cathepsin L	SPRi	Non fluidic	Slide /Au/ Array	1-octadecano-thiol / Inhibitor RKLW-NH2	Hydrophobic interaction	[34]

EDC/NHS: Covalent Amid Bond Formed Due to EDC/NHS Protocol; MoS2QDs@g-C3N4@CSAuNPs; g-C3N4: Graphitic Carbon Nitride; MoS2 QDs: Nanosheets and MoS2 Quantum Dots, followed by decoration with chitosan-stabilized Au nanoparticles; nd: No Data

procedure can be distinguished:

- i. The biosensor is used only for the detection of a marker;
- ii. The biosensor is characterized in terms of quantitative marker determination (calibration graph, the marker concentration range covered by the biosensor);
- iii. The biosensor and related analytical procedure are validated (precision, recovery, interferences, comparison of results with another procedure such as ELISA, examples of natural samples e.g. blood plasma);
- iv. The mature biosensor and the analytical procedure are used for investigation of the marker in significant series of clinical samples, including long control series of healthy donors;

The papers pertaining to stages i. and ii. represent incomplete analytical procedures. These papers represent high innovative potential in terms of biosensor construction, which may result in fully developed procedures in the future. The papers pertaining to stages iii. and iv. represent complete analytical procedures. These biosensors and related analytical procedures are ready to be subjected to clinical investigation for subsequent use in diagnosis. Additionally, biosensors in stage iv. are characterized as potential

disease markers by series of measurements performed with clinically classified material. Technical solutions for biosensors representing all four stages of development are shown in Tables 2 and 3, for cancer markers and other diseases respectively.

The number of fully developed biosensors (stages iii and iv) in Tables 1 and 2 outnumber those with incomplete analytical procedures (stages i and ii). This is a positive observation and a good prognostic factor for future SPR biosensors. This is a tendency corresponding to that recommended in the reviews by Masson and Ferhan et al. [14,15], and gives an indication of the future growing significance of SPR.

In the reviewed papers, classical SPR or SPR Imaging apparatus was used in the majority of cases. SPRi was frequently associated with non-fluidic measurement techniques. Occasionally, Localized SPR (LSPR) or Intensity-Modulated SPR (IM-SPR) were used. Instrumental differences between these versions of SPR are excellently reviewed in a paper by Wang et al. [50].

Fluidic vs. non-fluidic measurements

Approximately the same number of reviewed papers reported the use of fluidic and non-fluidic measurement technique. There is a significant difference in the arrangement of a fluidic or non-fluidic

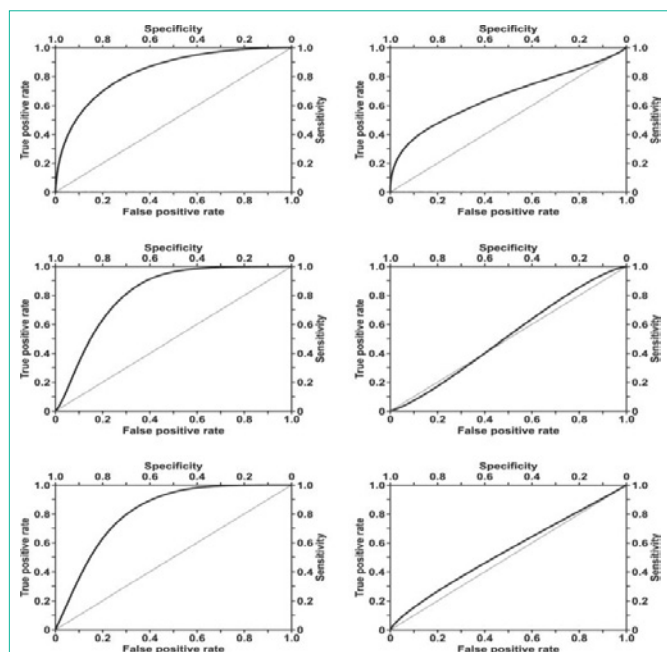


Figure 1: Diagnostic efficiency of podoplanin in serum (upper left) and podoplanin in urine (upper right) in the detection of bladder transitional cell carcinoma, podoplanin in serum (middle left) and podoplanin in urine (middle right) in the detection of invasive forms of bladder transitional cell carcinoma, and podoplanin in serum (lower left) and podoplanin in urine (lower right) in the detection of high risk of progression of bladder transitional cell carcinoma. Reproduced with permission from [1]. Copyright (2018) IOS Press.

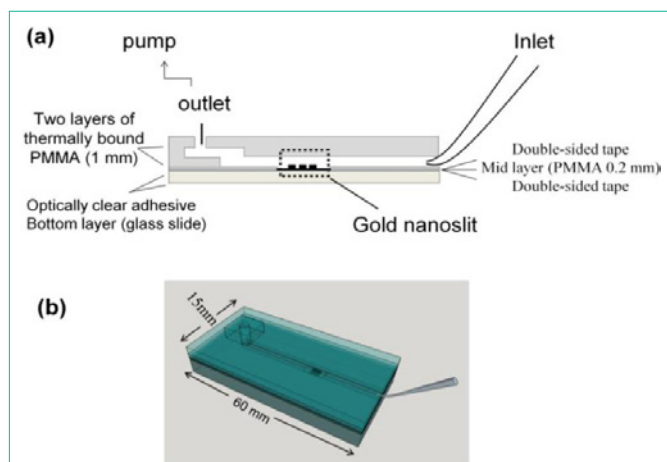


Figure 2: Example of a biosensor using a gold nanoslit substrate. Reproduced with permission from [51]. Copyright 2015, MDPI.

measurement: a fluidic measurement is usually performed with *in situ* creation of a biosensor, while in the non-fluidic case the biosensor is prepared *ex situ*. In the fluidic version measurement is performed with the biosensor in contact with solution. This is the major difference from the non-fluidic case. In the *in situ* version a biosensor is created during the measurement by sequential introduction of a linker, a receptor and a solution containing the determined marker. Finally, the chip sensor is cleaned to prepare it for the next measurement. Subsequent measurements can be performed rapidly, as in flow-injection analysis. A single biosensor usually contains several channels, processed simultaneously for multi-sample measurement

or for processing the same solution to gain better precision. The volume of processed solution also constitutes a difference between fluidic and microfluidic techniques: in the microfluidic case there is a tendency towards the miniaturization of the measuring process. Microfluidic measurement also uses an array of measuring points [17]. An example of such a solution is shown in Figure 2.

Non-fluidic measurement is usually performed in a stationary arrangement, with an array of separated measuring points. An example of non-fluidic measurement is shown in Figure 3. An array of measuring points is used for a single sample measurement to improve the precision of the result. Multi-sample measurement is also performed, as shown in Figures 3 and 4, as well as regeneration of the chip after measurement.

Non-fluidic *ex situ* SPR measurement is performed following gentle removal of solution from the biosensor surface, which is the major difference compared with fluidic measurements. No information has yet been published concerning the comparison of fluidic and non-fluidic versions of SPR measurements.

Receptors

A crucial part of a biosensor is the receptor. The receptor must ensure that only the target marker is captured from the analyzed sample, as well as ensuring suitable effectiveness in terms of the strength of analytical signal sufficient for the determination of a marker in real samples. In the reviewed papers, appropriate antibodies were most frequently used as receptors. The antibody was attached to the gold chip surface via a linker. Most frequently, cysteamine (2-aminoethanethiol) was used as the linker. Cysteamine is fixed onto the gold surface by the thiol group, while the amine group is used for attachment of the antibody. An example of such receptor immobilization is shown in Figure 4 left.

An EDC/NHS protocol is applied for this purpose, with amide bond formation between the antibody's carboxyl group and the linker's amine group. Alternatively, MUA (11-mercaptoundecanoic acid) may be used in conjunction with the EDC/NHS protocol [18]. The amine group of the antibody is used for the junction. Similarly, HS-OEG-COOH [51,52], S2PEG6COOH [19] (where OEG and PEG denote oxyethylene subunits) and mercapto propane sulfonate [36]

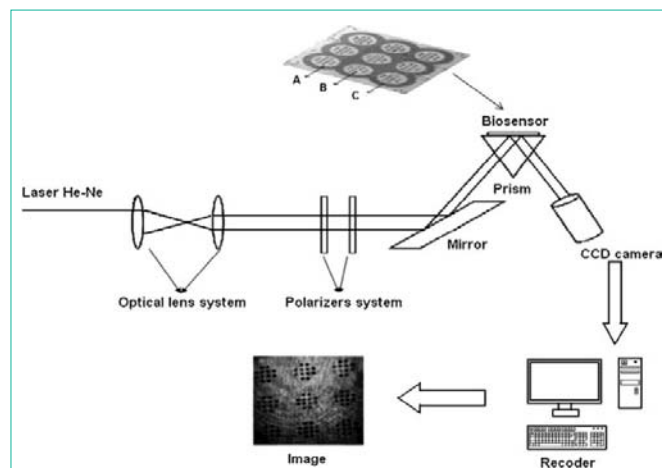


Figure 3: Example of non-fluidic measurement. Reproduced with permission from [49]. Copyright 2017 Elsevier B.V.

Table 3: Stages of biosensor development and technical solutions for biosensors used for the determination of various markers, excluding cancer markers.

Stage	Marker	SPR type	Fluidic/ Non fluidic	Chip	Linker /receptor	Receptor immobilization	Reference
i	BSA	SPR	Both	Prism/Au	Cysteamine/ GOCOOH/ /antibody mercapto propane sulfonate/ modified GO	EDC/NHS	[35]
i	BSA	SPR	Non fluidic	Slide/Au	Cysteamine/ GOCOOH/ /antibody mercapto propane sulfonate/ modified GO	EDC/NHS	[36]
i	Cytochrom C	SPRi	Fluidic	Easy2Spot	antibody	Sensor pre-activated G-type Senseye	[37]
i	ampicilin	EC-SPR	Fluidic	Slide/Cr/Au	thiolated aptamer	Aptamer/ /ampicilin	[38]
ii	Pf glutamate dehydro-genase	SPR	Fluidic	Au	thiolated aptamer	Thiolated aptamer	[39]
ii	Transferrin	SPR	Fluidic	Slide/Au	4-Mercapto phenylboronic	4-Mercapto phenylboronic	[40]
ii	Folic acid	SPR	Fluidic	Prism/Ti/ Au/graphene	FAP	Hydrophobic Interaction	[41]
iii	CBP	SPR	Fluidic	CM5 chip	Dextran-COOH/ Antibody	EDC/NHS	[42]
iii	Troponin T	SPR	Fluidic	Slide/Au	Polydopamine/ Epitop/	Polimer Imprinted epitop	[43]
iii	IgG	LSPR	Fluidic	photonic crystal fiber/ Au	Dithiothreitol/ antibody	EDC/NHS	[44]
iii	P. fijiensis	SPR	Fluidic	Prism/Cr/ Au	MHDA/antibody	EDC/NHS	[45]
iv	Avian Influenza A H7N9 Virus	IM-SPR	Non fluidic	Ag/Au	MUA/antibody	EDC/NHS	[46]
iv	YKL40	SPR	Fluidic	CM5 chip	Dextran-COOH/ Antibody	EDC/NHS	[47]
iv	Mortalin & α -Synuclein	SPR	Fluidic	CM5 chip	Dextran-COOH/ Antibody	EDC/NHS	[48]
iv	Fibronectin	SPRi	Non fluidic	Slide/Au	Cysteamine/ Antibody	EDC/NHS	[49]

EDC/NHS: Covalent Amid Bond Formed Due to EDC/NHS Protocol; IM-SPR: Intensity-Modulated SPR; MHDA: 16-Mercaptohexadecanoic Acid; P. fijiensis: fungus *Pseudocercospora fijiensis*

have been used. In numerous papers, the commercially available CM5 chip with carboxylated dextran as the linker was employed. Another commercially available chip (Easy2Spot) is supplied in a form ready for antibody bonding [37].

Several solutions other than antibodies have been used as receptors. A marker's inhibitor can be used as the receptor, as in the cases of the inhibitor ONX 0914 [32] and the inhibitor ARP 101 [33]; in both cases 1-octadecano-thiol was used as the linker, and the inhibitor was attached to the linker via hydrophobic interactions. An example of this type of receptor immobilization is shown in Figure 5 right.

Tionylated aptamer targeting analyte is also used as a receptor [23,38,39]. In such a case no linker is used. A receptor-imprinted polymer may also be used as the receptor [25,43].

A glass slide covered with gold is a typical chip base (Figure 4). Alternatively, a gold-covered glass prism is used. Usually, a chromium—or alternatively, titanium—under-layer is employed. Only a few papers report other solutions, such as a gold-covered glass fiber [19], also with additional graphene layer [53], a gold nanohole array [17,54], or a gold nanoslit substrate [51] or a prism covered with gold and graphene [55]. Frequently, a gold chip surface is covered by a polymer with holes, creating an array of free gold measuring points (Figures 3 and 4). A thick inert polycarbonate protective layer is also proposed [56].

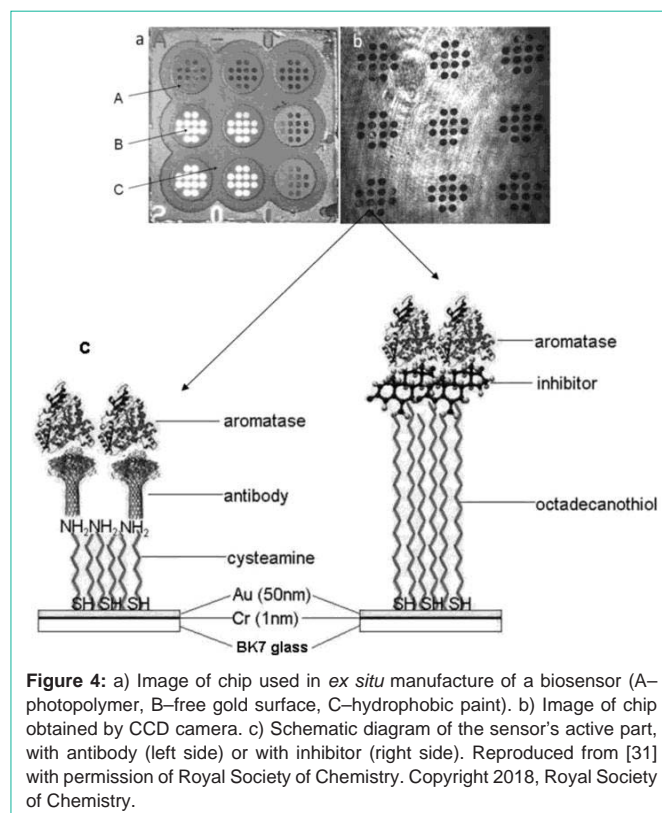


Figure 4: a) Image of chip used in *ex situ* manufacture of a biosensor (A-photopolymer, B-free gold surface, C-hydrophobic paint). b) Image of chip obtained by CCD camera. c) Schematic diagram of the sensor's active part, with antibody (left side) or with inhibitor (right side). Reproduced from [31] with permission of Royal Society of Chemistry. Copyright 2018, Royal Society of Chemistry.

Table 4: Stages of biosensor development and technical solutions for biosensors with the use of nanoparticles.

Stage	Marker	SPR type	Fluidic/ Non fluidic	Chip/NP	Sandwich/ /other	receptors immobilization (chip/NP)	Reference
ii	miRNA141	SPR	Non fluidic	Au/DNA AuNPMoS2	sandwich	Thionylated DNA/DNA linked AuNPMoS2	[61]
ii	miRNA141	SPR	Non fluidic	Au/DNA GO–AuNP	sandwich	Thionylated DNA/DNA linked GO–AuNP	[62]
ii	Folic acid	SPRi	Non fluidic	Array/Cr/Au/ FA–AuNP	Sandwich	HS–(CH2)11– EG3–NTA/polyhistidine	[41]
ii	Troponin I	SPR	fluidic	Slide/Au/ /HGNNP/ MMWCNTs–PDA	Sandwich/ / MMWCNTs–PDA	Polydopamine/ Polydopamine	[60]
ii	PSA	SPR	fluidic	AuNP/CS/ /C3N4/ /MoS2QD	Multi-component structure	nanosheet/ /aptamer	[23]
ii	Rabbit IgG	SPR	nd	Slide/Au/ /HGNNP	sandwich	1,6-hexanedithiol/ /PDA–Ag@Fe3O4/ rGO	[63]
ii	Prion Sc protein	SPR	Fluidic	Slide/Au/ / Fe3C@C	sandwich	?/ Fe3C@C–aptamer	[64]
ii	miRNA200	SPR	nd	Prism/Au/ AuNP–surrogate DNA	Sandwich–competition	MUA/ surrogate DNA/	[65]
iii	CEA	SPR	fluidic	Slide/Ti/Au /AuNP	Sandwich	HS–OEG–COOH/ HS–OEG–COOH/ EDC/NHS	[52]
iii	HER 2	SPR	Micro–fluidic	Prism/Au/ SAV–GNPs	Sandwich	MUA/ EDC/NHS/ biotinylated antibody	[57]
iii	IgG	LSPR	Fluidic	photonic crystal fiber/Au/ AuNP	other	Dithiothreitol/EDC/NHS/antibody	[44]
iii	IgG	LSPR	Fluidic	photonic crystal fiber/Au/ AuNP/protein A	other	Dithiothreitol/EDC/NHS/protein A/ antibody	[44]
iii	cTnI	SPR	Fluidic	Slide Au/ PDA/AuNP/ /antibody1	Sandwich/ /MMP/PDA/ /antibody1	PDA	[66]
iii	cTnI	SPR	Fluidic	Sandwich/ /MMP/PDA/ /antibody1	Sandwich//MMP/PDA/ /antibody1/ MWCNTs–PDA– AgNPs/antibody2	PDA	[66]
iv	Cytochrom C	SPR	fluidic	Slide/Au /AuNR	Sandwich/ /MMP	Straptavidin/ /biotinylated aptamer/ /antibody/MMP	[58]
iv	AFP, CEA CYFRA 21-1	SPR	Micro–fluidic	Prism/Au	Sandwich/ /QD	Hexanedithiol/ /antibody/ DTBE	[59]

SAV–GNPs: Streptavidin Decorated Gold Nanoparticles; FA–AuNP: AuNP Functionalized with Polyhistidine Tagged Folic Acid Binding Protein; AuNR: Au Nanorods; MMP: Micro Magnetic Particles; QD: Quantum Dot (CdSe/ZnS core/shell structure); DTBE - 2,2': Dithiobis[1-(2-Bromo-2-Methylpropionyloxy)]Ethane; AFP: α-Fetoprotein; MMWCNTs–PDA: Polydopamine–Wrapped Magnetic Multi–Walled Carbon Nanotubes; HGNNP: Hollow Gold Nanoparticles; MoS2QDs@g–C3N4@CS–AuNPs: Graphitic Carbon Nitride (g–C3N4) Nanosheets and MoS2 QDs: MoS2 Quantum Dots
 Followed by decoration with chitosan–stabilized Au nanoparticles
 PDA–Ag@Fe3O4/rGO: Polydopamine–Ag@Fe3O4/reduced Graphene Oxide; DNAAuNPMoS2: DNA–Linked AuNPs–MoS2 Hybrids; GO–AuNP: Graphen Oxide – Au Nanoparticles Hybrid; nd: No data

Enhancement of the SPR signal

As demonstrated by Brolo’s research group in Canada, periodic areas of nanoholes in a sandwich configuration may be used to enhance the SPR signal [17]. The first antibody captures the marker, while the marker captures the second antibody. The introduction of different nanoparticles in the sandwich can lead to much greater enhancement of the SPR signal. Table 4 summarizes the cases in which nanoparticles were applied. In the simplest solution, the first antibody attached by the EDC/NHS protocol captures the marker, which captures an aggregate consisting of a gold nanoparticle covered by a second antibody attached to the antibody surface by the same EDC/NHS protocol [52]. A similar solution is reported [57] in which the EDC/NHS protocol is used for the first antibody attachment, and a biotinylated antibody attached to streptavidin–decorated gold nanoparticles serves as the second. The preconcentration of the marker with magnetic microparticles covered by the antibody has been reported [58]. Finally, the signal is created indirectly by a selected aptamer released from the magnetic microparticles–antibody–marker–aptamer structure. A quantum dot having CdSe/ZnS core/

shell structure has also been used for SPR signal enhancement in a sandwich configuration [59], as have polydopamine–wrapped magnetic multi–walled carbon nanotubes [60]. Two very efficient signal enhancement procedures have been used for the determination of microRNA–141 [61,62]. Gold nanoparticle–decorated molybdenum sulfide containing thiol–modified DNA oligonucleotide probes, having a sequence complementary to the target miRNA–141, was attached to the Au film containing the segment sequence of the target miRNA–141 by means of the miRNA–141 [61]. Similarly, a graphene oxide–gold nanoparticle hybrid with attached thiol–modified DNA oligonucleotide probe was used [62].

Calibration strategy

In our opinion, the most significant information concerning the calibration strategy is whether the range of measurable concentration covers the range of concentrations of the marker in cancer samples and a representative level for the healthy population. In some cases, the reported dynamic response range covers several orders of magnitude (e.g. [52]). However, linearity of the analytical response is obtained when the analytical signal is plotted against log marker

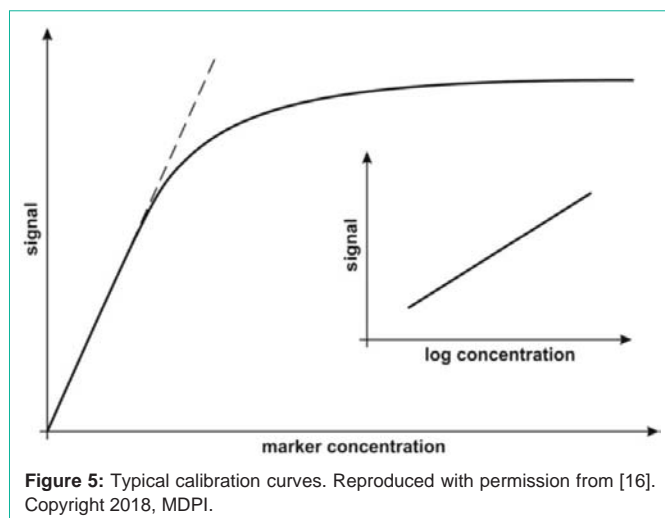


Figure 5: Typical calibration curves. Reproduced with permission from [16]. Copyright 2018, MDPI.

concentration. In other cases, linearity of the analytical signal against the marker concentration is reported, but in a significantly narrower concentration range. Generally, all calibration graphs represent the Langmuirian curve type, in which the initial sections may approximately follow the strain lines, while the whole curve may be approximately linear when the analytical signal is plotted against log marker concentration (Figure 5). Almost all of the reviewed papers containing calibration data report calibration on the basis of a linear calibration graph. Only two papers refer to semi-log calibration [22,42]. This appears to be a reasonable choice, because determination of the logarithm of the marker concentration does not satisfy expectations for clinical results.

Molecular markers

In the reviewed papers, the targets of the developed—or merely applied—biosensors are various types of cancer, as well as other diseases. These targets are listed in Table 5. Lung, bladder and breast cancers are most frequently represented. Single papers have been devoted to colorectal, prostate, and head and neck squamous cell cancers, as well as acute leukaemia. Among non-cancer applications, thermal injuries have been most frequently investigated, as well as acute myocardial infarction and acute appendicitis. Papers devoted to apoptosis, asthma, megaloblastic anemia, Parkinson's disease, hypertension, primary renal disease and diabetes have also been published. Some biosensors have found applications with several diseases; for example, 20 S proteasome and UCHL1. In the majority of cases, the biosensors were used for the determination of markers in the blood serum or plasma, although in several cases urine was the target body fluid.

Other circulating markers

Micro RNAs (miRNAs) are non-coding RNAs regulating gene expression through base-pairing with complementary sequences of messenger RNA (mRNA) molecules. As a result, these mRNA molecules are silenced. miRNAs are small molecules containing approximately 22 nucleotides. They are emerging cancer markers [67,68]. The detection of miRNA by SPR requires signal amplification, due to the small size of the molecules, which results in a low SPR signal. Various approaches are used to amplify the miRNA signal in SPR. Hong et al. [65] developed a competition assay for the

determination of miRNA 200b. The SPR analytical signal is created by the replacement of gold nanoparticles conjugated with surrogate DNA by the analyte (miRNA 200b). The conjugated nanoparticles are attached to the biosensor surface by a suitable DNA via MUA linker. Wang et al. [62] used graphene oxide–gold nanoparticle hybrids for miRNA141 SPR signal enhancement. Two thiol-modified DNA oligonucleotide probes, containing sequences complementary to the target miRNA-141, were used; the capture DNA was immobilized on a gold sensor surface, while the other (called assistant DNA) was fixed on the graphene oxide–gold nanoparticle hybrids. These hybrids were used for signal amplification. One section of the miRNA-141 is bound to the capture DNA, while the other section is bound to the assistant DNA, forming a sandwich structure. The developed method ensures highly sensitive and selective miRNA-141 determination in prostate carcinoma cell lines (22Rv1), hepatocellular carcinoma cell lines (SMMC-7721), colon cancer cell lines (LoVo), and cervical cancer cell lines (HeLa). A similar solution was applied by Nie et al. [61] for miRNA-141 determination in the cell lysates from cancer cell lines 22Rv1, SMMC-7721, LoVo and HeLa. Li et al. [63] used mismatched catalytic hairpin assembly amplification coupling with programmable streptavidin aptamer for miRNA-21 determination. Two hairpin DNAs were used.

Exosomes are emerging biomarkers. These small extracellular vesicles, secreted by cells, are present in body fluids (blood, urine, breast milk, saliva) and transfer DNAs, RNAs, proteins, and lipids from parent cells to recipient cells for cell-cell communication. Exosomes are involved in the regulation of immune responses and in cancer development. There are several papers on SPR determination of exosomes as potential cancer or heart disease markers. Zhu et al. [69] applied antibody microarrays specific to the extracellular domains of exosome membrane proteins in a fluidic system in conjunction with the SPRi technique.

Park et al. [70] applied nanohole-based surface plasmon resonance for the detection of transmembrane (EpCAM and CD63) and intravesicular (AKT1) proteins contained in exosomes' lysates. The exosomes originated from three ovarian cancer cell lines and one benign cancer cell line. Apart from the atypical nanohole SPR, which is more sensitive than usual SPR, gold nanoparticles were used to enhance the analytical signal.

Ibn Sina et al. [71] used a custom-made fluidic SPR platform for quantification of the proportion of cancer-related exosomes within the total exosome population isolated from patient serum, which may potentially provide information on the stage of the disease. A two-step strategy was applied, involving initial isolation of the total exosome population using tetraspanin biomarkers (CD9, CD63) and subsequent detection of exosomes containing the HER2 marker (breast cancer) by the formation of a sandwich with anti-HER2.

Reiner et al. [72] used a magnetic nanoparticle-enhanced grating coupled SPR assay for specific detection of different small lipid extracellular vesicles secreted from mesenchymal stem cells. Pre-incubated vesicles were captured by magnetic nanoparticles via lipid-binding annexin V and cholera toxin B chain immobilized on the nanoparticles' surface. An antibody specific for the tetraspanin protein CD63 was used for sensitive detection of extracellular vesicles.

Unlike the previously cited papers, which all concern cancer

Table 5: Molecular markers and related diseases.

Marker	Abbrev.	Cancer /or other disease	Body fluid	Reference
Arachidonate 5- lipoxygenase	5LOX/ ALOX5	Breast cancer	Blood plasma	[27]
Carcinoembryonic antigen	CEA	Colorectal cancer	Blood serum	[18]
Calcium Binding Protein	CBP	Acute myocardial infarction	Blood serum	[42]
Cathepsin B	Cath B	Appendicitis	Blood plasma	[11]
Chitinase-3-like protein 1	CHI3L1/ YKL-40	Asthma	Blood serum	[47]
Collage IV		Breast cancer/ burns	Blood serum	[30]
Cyclin-dependent kinase 4	CDK4	Lung, head and neck cancers	Blood serum	[28]
Cystatin C		Bladder cancer	Blood serum, urine	[3]
Cytochrom C		Apoptosis	No information	[37]
Cytokeratin 17	CK 17	Lung cancer	No information	[19]
Cytokeratin 19	CK19	Lung cancer	Blood plasma	[35]
Epidermal receptor protein-2 antigen	HER	Breast cancer	No information	[17]
Fibronectin		Burns	Blood plasma	[49]
Folic acid	FA	Megaloblastic anemia	Blood	[41]
20S-immunoproteasom	20Si	Acute leukemia	Blood plasma	[32]
20S Immunoproteasom	20Si	Burns	Blood plasma	[67]
Laminin 5		Bladder cancer/burns	Blood plasma	[5,29]
Matrix metalloproteinase-1	MMP1	Bladder cancer/ acute appendicitis	Blood serum	[31]
Matrix metalloproteinase-2	MMP2	Burns	Blood plasma	[5,33]
Mortalin/mitochondrial 70kDa heat shock protein,	mtHsp70	Parkinson's Disease	Blood serum	[48]
Podoplanin		Bladder cancer	Blood serum, urine	[1]
20S-proteasom	20Sc	Burns, acute appendicitis, Cryptorchidism	Blood plasma	[7]
Prostate specific antigen	PSA	Prostate cancer	Blood serum	[25]
Ras-related C3 botulinum toxin substrate 1	Rac1	Non Small Cell Lung Cancer	Blood serum	[26]
Ras-related C3 botulinum toxin substrate 1b	Rac1b	Non Small Cell Lung Cancer	Blood serum	[26]
Transferrin	Trf	Hypertension, primary renal disease, diabetes.	Artificial urine	[40]
Troponin T	TnT	Acute myocardial infarction	Blood serum	[16]
Ubiquitin carboxyl-terminal hydrolase L1	UCHL1	Burns, Cryptorchidism, Acute Appendicitis	Blood serum	[10] [4] [8]

detection, Hosseinkhani et al. [73] report on the use of extracellular vesicles as a potential heart disease marker. As in the previous papers, an antibody specific for the tetraspanin protein CD63 was used for the sensitive detection of extracellular vesicles, and anti- ICAM-1 (Intercellular Adhesion Molecule 1) for the detection of captured vesicles related to coronary heart disease.

Circulating Tumor Cells (CTCs) are also potential cancer markers. They are released from the cancer into the blood. However, the concentration of CTCs in blood is extremely low. Therefore, CTC accumulation is applied, as well as SPR signal enhancement. Mousavi et al. [51] used a gold nanoslit SPR platform for sensitive detection of the lung cancer cell lines CL1–5. The CL1–5 cells were initially accumulated on functionalized magnetic nanoparticles.

Jia et al. [74] detected the breast cancer cell line MCF-7 using histidine-tagged arginine-glycine-aspartic acid peptide as a linker. The breast cancer cells MCF-7 were captured via the interaction

between human mucin-1 and a gold surface modified with a mucin-1-selective aptamer. The SPR signal was enhanced by binding of NiO nanoparticles via the histidine tag on the peptide.

Molecular interactions

Apart from the papers devoted to the determination of particular markers in body fluids, there are a number of papers on SPR describing investigations of molecular interactions (Table 6). One of these [75] describes the interactions of immobilized Cancer Antigen 125 (CA 125) with several aptamers. Elsewhere, the interaction between recombinant Smurf2 protein and CNKSR2 protein was described [76]. Other studies have investigated the parameters of binding between galectin-3 and pectin [77] and the glycosylation-dependent binding of galectin-8 to Activated Leukocyte Cell Adhesion Molecule (ALCAM) [78]. A further study [79] investigated the affinity and competitive inhibition of nine Caffeoylquinic Acid compounds (CQAs) against programmed cell death Protein 1

Table 6: Examples of applications of SPR biosensors in the investigation of intermolecular interactions.

Interaction of	with	Reference
CA 125	aptamers	[75]
recombinant Smurf2 protein	CNKS2 protein	[76]
galectin-3	pectin	[77]
galectin-8	ALCAM	[78]
caffeoylquinic acids	PD-1	[79]
PSA	lectins	[80]
NTV1	VEGFR2 D3	[81]
GP2	VHH	[82]
Tau protein	aptamers	[83]
HIV-1 gp120	antibody fragments (ScFab or ScFv)	[86]
Angiotensin converting enzyme	potential inhibitors	[84]
Porcine mucin	tannins	[85]

CA 125: Cancer Antigen 125; ALCAM: Activated Leukocyte Cell Adhesion Molecule; PD-1: Programmed Cell Death Protein 1; NTV1: Nanobody-Targeting VEGFR; GP2: Zymogen-Granule Membrane Glycoprotein 2; VHH: Camelid Recombinant Single Domain Antibodies

(PD-1) and its ligand PD-L1. Another investigation concerned the binding affinities of prostate-specific antigen to six lectins [80], and elsewhere, the ability of Nanobody-Targeting VEGFR (NTV1) to bind VEGFR2 D3 was demonstrated [81]. The binding kinetics of camelid recombinant single domain antibodies to immobilized zymogen-granule membrane glycoprotein 2 were investigated [82], as well as the interaction of tau protein with different aptamers [83]. Potential inhibitors of angiotensin converting enzyme were sought via screening of medicinal plants [84]. Gombau et al. [85] investigated interactions between porcine mucin and tannins. Binding studies of refolded single chain antibody fragments with HIV-1 gp120 were performed by Singh [86]. Generally, the aim of these papers is to investigate different drugs and therapies.

Conclusion

A majority of the reviewed papers represent validated biosensors and related analytical procedures. Numerous papers were devoted to clinical investigations with cancer markers and other diseases as the targets of biosensors. The calibration strategy was generally based on straight line calibration curves, although semi-logarithmic curves were also used. Antibodies were the most frequently used type of receptors. Some of the reviewed papers used fluidic measurement arrangements, while others used stationary non-fluidic measurement with an array of measuring points.

Acknowledgement

The authors are grateful to IOS Press for giving permission to reproduce Figure 1, to MDPI for Figures 2 and 5, to Elsevier BV for Figure 3, and to the Royal Society of Chemistry for Figure 4.

References

- Sankiewicz A, Guszcz T, Mena-Hortelano R, Zukowski K, Gorodkiewicz E. Podoplanin serum and urine concentration in transitional bladder cancer. *Cancer Biomark*. 2016; 16: 343-350.
- Matuszczak E, Tylicka M, Hermanowicz A, Debek W, Sankiewicz A, Gorodkiewicz E. Application of SPR imaging biosensor for the measurement of 20S proteasomes in blood plasma of children with thermal injury. *Anal Clin Lab Sci*. 2016; 46: 407-411.
- Tokarzewicz A, Guszcz T, Onopiuk A, Kozłowski R, Gorodkiewicz E. Utility of cystatin C as a potential bladder tumour biomarker confirmed by surface plasmon resonance technique. *Indian J A Med Res*. 2018; 218: 46-50.
- Matuszczak E, Tylicka M, Debek W, Sankiewicz A, Gorodkiewicz E, Hermanowicz A. Overexpression of ubiquitin carboxyl-terminal hydrolase L1 (UCHL1) in serum of children after thermal injury. *Adv Med Sci*. 2017; 62: 83-86.
- Weremijewicz A, Matuszczak E, Sankiewicz A, Tylicka M, Komarowska M, Tokarzewicz A, et al. Matrix metalloproteinase-2 and its correlation with basal membrane components laminin-5 and collagen type IV in pediatric burn patients measured with Surface Plasmon Resonance Imaging (SPRI) biosensors. *Burns*. 2018; 44: 931-940.
- Toliczenko-Bernatowicz D, Matuszczak E, Tylicka M, Szymańska B, Komarowska M, Gorodkiewicz E, et al. Overexpression of ubiquitin carboxyl-terminal hydrolase 1 (UCHL1) in boys with cryptorchidism. *Plos One*. 2018; 13: e0191806.
- Matuszczak E, Tylicka M, Debek W, Sankiewicz A, Gorodkiewicz E, Hermanowicz A. Concentration of Proteasome in the Blood Plasma of Children with Acute Appendicitis, Before and After Surgery, and Its Correlation with CRP. *World J Surg*. 2018; 42: 2259–2264.
- Matuszczak E, Tylicka M, Debek W, Tokarzewicz A, Gorodkiewicz E, Hermanowicz A. Concentration of UHCL1 in the Serum of Children with Acute Appendicitis, Before and After Surgery, and Its Correlation with CRP and Prealbumin. *J Investig Surg*. 2018; 31: 136-141.
- Toliczenko-Bernatowicz D, Matuszczak E, Tylicka M, Sankiewicz A, Komarowska M, Gorodkiewicz E, et al. 20S proteasome in the blood plasma of boys with cryptorchidism. *J Endocrinol Investig*. 2018; 41: 1103–1106.
- Matuszczak E, Sankiewicz A, Debek W, Gorodkiewicz E, Milewski R, Hermanowicz A. Immunoproteasome in the blood plasma of children with acute appendicitis, and its correlation with proteasome and UCHL1 measured by SPR imaging biosensors. *Clin Exper Immun*. 2018; 191: 125-132.
- Matuszczak E, Komarowska M, Tylicka M, Debek W, Gorodkiewicz E, Tokarzewicz A, et al. Determination of the concentration of cathepsin B by SPRI biosensor in children with appendicitis, and its correlation with proteasomes. *Adv Clin Exp Med*. 2018; 27: 1529–1534.
- GrzywaR, GorodkiewiczE, Burchacka E, Lesner A, Laudanski P, Lukaszewski Z, et al. Determination of cathepsin G in endometrial tissue using a surface plasmon resonance imaging biosensor with tailored phosphonic inhibitor. *Eur J Obstet Gynecol Reprod Biol*. 2014; 182: 38–42.
- Laudanski P, Gorodkiewicz E, Ramotowska B, Charkiewicz R, Kuzmicki M, Szamatowicz J. Determination of cathepsins B, D and G concentration in eutopic proliferative endometrium of women with endometriosis by the surface plasmon resonance imaging (SPRI) technique. *Eur J Obstet Gynecol Reprod Biol*. 2013; 169: 80–83.
- Masson JF. Surface Plasmon Resonance Clinical Biosensors for Medical Diagnostics. *ACS Sens*. 2017; 2: 16-30.
- Ferhan AR, Jackman JA, Park JH, Cho NJ, Kim DH. Nanoplasmonic sensors for detecting circulating cancer biomarkers. *Adv Drug Deliv Rev*. 2018; 125: 48–77.
- Gorodkiewicz E, Lukaszewski Z. Recent Progress in Surface Plasmon Resonance Biosensors (2016 to Mid-2018). *Biosensors*. 2018; 8: 132.
- Monteiro JP, de Oliveira JH, Radovanovic E, Brolo AG, Girotto EM. Microfluidic Plasmonic Biosensor for Breast Cancer Antigen Detection. *Plasmonics*. 2016; 11: 45–51.
- Xu J, Chen Y. Surface plasmon resonance sensing with adjustable sensitivity based on a flexible liquid core coupling unit. *Talanta*. 2018; 184: 468-474.
- Ribaut C, Loyez M, Larrieu JC, Chevigneau S, Lambert P, Rimmelink M, et al. Cancer biomarker sensing using packaged plasmonic optical fiber gratings: Towards *in vivo* diagnosis. *Biosens Bioelectron*. 2017; 92: 449-456.
- Vergara D, Bianco M, Pagano R, Priore P, Lunetti P, Guerra F, et al. An

- SPR based immunoassay for the sensitive detection of the soluble epithelial marker E-cadherin. *Nanomedicine: Nanotechnol Biol Med.* 2018; 14: 1963-1971.
21. Teotia PK, Kaler RS. 1-D grating based SPR biosensor for the detection of lung cancer biomarkers using Vroman effect. *Optics Communic.* 2018; 406: 188-191.
22. Chiu N-F, Lin TL, Kuo CT. Highly sensitive carboxyl-graphene oxide-based surface plasmon resonance immunosensor for the detection of lung cancer for cytokeratin 19 biomarker in human plasma, *Sens. Actuators B*, 2018; 265: 264-272.
23. Duan F, Zhang S, Yang L, Zhang Z, He L, Wang M. Bifunctional aptasensor based on novel two-dimensional nanocomposite of MoS₂ quantum dots and g-C₃N₄ nanosheets decorated with chitosan-stabilized Au nanoparticles for selectively detecting prostate specific antigen. *Anal Chim Acta.* 2018; 1036: 121-132.
24. Loyez M, Albert J, Caucheteur C, Wattiez R. Cytokeratins Biosensing Using Tilted Fiber Gratings. *Biosensors.* 2018; 8: 74.
25. Erturk G, Ozen H, Tumer MA, Mattiasson B, Denizli A. Microcontact imprinting based surface plasmon resonance (SPR) biosensor for real-time and ultrasensitive detection of prostate specific antigen (PSA) from clinical samples. *Sens. Actuators, B.* 2016; 224: 823-832.
26. Sahu V, Gupta A, Kumar R, Gupta T, Mohan A, Dey S. Quantification of Rac1 and Rac1b in serum of non small cell lung cancer by label free real time assay. *Clin Chim Acta.* 2016; 460: 231- 235.
27. Kumar R, Singh AK, Kumar M, Shekhar S, Rai N, Kaur P, et al. Serum 5-LOX: a progressive protein marker for breast cancer and new approach for therapeutic target. *Carcinogenesis.* 2016; 37: 912-917.
28. Banerjee J, Pradhan R, Gupta A, Kumar R, Sahu V, Upadhyay AD, et al. CDK4 in lung, and head and neck cancers in old age: evaluation as a biomarker. *Clin Transl Oncol.* 2017; 19: 571-578.
29. Sankiewicz A, Romanowicz L, Laudanski P, Zelazowska-Rutkowska B, Puzan B, Cylwik B, et al. SPR imaging biosensor for determination of laminin-5 as a potential cancer marker in biological material. *Anal Bioanal Chem.* 2016; 408: 5269-5276.
30. Sankiewicz A, Lukaszewski Z, Trojanowska K, Gorodkiewicz E. Determination of collagen type IV by Surface Plasmon Resonance Imaging using a specific biosensor. *Anal Biochem.* 2016; 515: 40-46.
31. Tokarzewicz A, Romanowicz L, Sveklo I, Gorodkiewicz E. The development of a matrix metalloproteinase-1 biosensor based on the surface plasmon resonance imaging technique. *Anal Methods.* 2016; 8: 6428-6435.
32. Sankiewicz A, Markowska A, Lukaszewski Z, Puzan B, Gorodkiewicz E. Methods for 20S Immunoproteasome and 20S Constitutive Proteasome Determination Based on SPRI Biosensors. *Cell Molec Biol Engine.* 2017; 10: 174-185.
33. Tokarzewicz A, Romanowicz L, Sveklo I, Matuszczak E, Hermanowicz A, Gorodkiewicz E. SPRI biosensors for quantitative determination of matrix metalloproteinase-2. *Anal Methods.* 2017; 9: 2407-2414.
34. Tokarzewicz A, Romanowicz L, Sankiewicz A, Hermanowicz A, Sobolewski K, Gorodkiewicz E. A New Analytical Method for Determination of Cathepsin L Based on the Surface Plasmon Resonance Imaging Biosensor. *Int J Mol Sci.* 2019; 20: 2166.
35. Chiu NF, Fan SY, Yang CD, Huang TY. Carboxyl-functionalized graphene oxide composites as SPR biosensors with enhanced sensitivity for immunoaffinity detection. *Biosens Bioelectron.* 2017; 89: 370-376.
36. Primo EN, Bollo S, Rubianes SMD, Rivas GA. Immobilization of graphene-derived materials at gold surfaces: Towards a rational design of protein-based platforms for electrochemical and plasmonic applications. *Electrochim Acta.* 2018; 259: 723-732.
37. Stojanović I, van Hal Y, van der Velden TJG, Schasfoort RBM, Terstappen LWMM. Detection of apoptosis in cancer cell lines using Surface Plasmon Resonance imaging. *Sensing Bio-Sens Res.* 2016; 7: 48-54.
38. Blidar A, Feier B, Tertis M, Galatus R, Cristea C. Electrochemical surface plasmon resonance (EC-SPR) aptasensor for ampicillin detection. *Anal Bioanal Chem.* 2019; 411: 1053-1065.
39. Singh NK, Arya SK, Estrela P, Goswami P. Capacitive malaria aptasensor using Plasmodium falciparum glutamate dehydrogenase as target antigen in undiluted human serum. *Biosens Bioelectron.* 2018; 117: 246-252.
40. Mayang Y, He X, Chen L, Zhang Y. Detection of transferrin by using a surface plasmon resonance sensor functionalized with a boronic acid monolayer. *Microchim Acta.* 2017; 184: 2749-2757.
41. Cao Y, Griffith B, Bhomkar P, Wishart DS, McDermott MT. Functionalized gold nanoparticle-enhanced competitive assay for sensitive small-molecule metabolite detection using surface plasmon resonance. *Analyst.* 2018; 143: 289-296.
42. Kim DH, Cho IH, Park JN, Paek SH, Cho HM, Paek SH. Semi-continuous, real-time monitoring of protein biomarker using a recyclable surface plasmon resonance sensor. *Biosens Bioelectron.* 2017; 88: 232-239.
43. Palladino P, Minunni M, Scarano S. Cardiac Troponin T capture and detection in real-time via epitope-imprinted polymer and optical biosensing. *Biosens Bioelectron.* 2018; 106: 93-98.
44. Wang BT, Wang Q. Sensitivity-Enhanced Optical Fiber Biosensor Based on Coupling Effect Between SPR and LSPR. *IEEE Sensors J.* 2018; 18: 8303-8310.
45. Luna-Moreno D, Sánchez-Álvarez A, Islas-Flores I, Canto-Canche B, Carrillo-Pech M, Villarreal-Chiu JF, et al. Early Detection of the Fungal Banana Black Sigatoka Pathogen *Pseudocercospora fijiensis* by an SPR Immunosensor Method. *Sensors.* 2019; 19: 465.
46. Chang YF, Wang WH, Hong YW, Yuan RY, Chen KH, Huang YW, et al. Simple Strategy for Rapid and Sensitive Detection of Avian Influenza A H7N9 Virus Based on Intensity-Modulated SPR Biosensor and New Generated Antibody. *Anal Chem.* 2018; 90: 1861-1869.
47. Naglot S, Aggarwal P, Dey S, Dalal K. Estimation of Serum YKL-40 by Real-Time Surface Plasmon Resonance Technology in North-Indian Asthma Patients. *Clin Lab Anal.* 2017; 31: e22028.
48. Singh AP, Bajaj T, Gupta D, Singh SB, Chakrawarty A, Goyal V, et al. Serum Mortalin Correlated with α Synuclein as Serum Markers, in Parkinson's Disease: A Pilot Study. *Neuro Molec Med.* 2018; 20: 83-89.
49. Sankiewicz A, Romanowicz L, Pyc M, Hermanowicz A, Gorodkiewicz E. SPR imaging biosensor for the quantitation of fibronectin concentration in blood samples. *J Pharm Biomed Anal.* 2018; 150: 1-8.
50. Wang D, Loo JFC, Chen J, Yam Y, Chen SC, He H, et al. Recent Advances in Surface Plasmon Resonance Imaging Sensors. *Sensors.* 2019; 19: 1266.
51. Mousavi MZ, Chen HY, Hou HS, Chang CYY, Roffler S, Wei PK, et al. Label-Free Detection of Rare Cell in Human Blood Using Gold Nano Slit Surface Plasmon Resonance. *Biosensors.* 2015; 5: 98-117.
52. Springer T, Chadová Song X, Ermini ML, Lamačová J, Homola J. Functional gold nanoparticles for optical affinity biosensing. *Anal Bioanal Chem.* 2017; 409: 4087-4097.
53. Zhang NMY, Li K, Shum PP, Yu X, Zeng S, Wu Z, et al. Hybrid graphene/gold plasmonic fiber-optic biosensor. *Adv Mater Technol.* 2017; 2: 1600185.
54. Blanchard-Dionne AP, Meunier M. Multiperiodic nanohole array for high precision sensing. *Photonics.* 2018; 5: 15.
55. He L, Pagneux Q, Larroulet I, Serrano AY, Pesquera A, Zurutuza A, et al. Label-free femtomolar cancer biomarker detection in human serum using graphene-coated surface plasmon resonance chips. *Biosens Bioelectron.* 2017; 89: 606-611.
56. Rizal T. Magneto-Optic Surface Plasmon Resonance Ti/Au/Co/Au/Pc Configuration and Sensitivity. *Magnetochem.* 2018; 4: 35.
57. Eletxigerra U, Martinez-Perdiguero J, Barderas R, Pingarron JM, Campuzano S, Merino S. Surface plasmon resonance immunosensor for ErbB2 breast cancer biomarker determination in human serum and raw cancer cell lysates. *Anal Chim Acta.* 2016; 905: 156-162.

58. Loo J FC, Yang C, Tsang HL, Lau PM, Yong KT, Ho HP, et al. An Aptamer Bio-barCode (ABC) assay using SPR, RNase H, and probes with RNA and gold-nanorods for anti-cancer drug screening. *Analyst*. 2017; 142: 3579-3587.
59. Wang H, Wang X, Wang J, Fu W, Yao C. A SPR biosensor based on signal amplification using antibody-QD conjugates for quantitative determination of multiple tumor markers. *Sci Reports*. 2016; 6: 33140.
60. Wu Q, Sun Y, Zhang D, Li S, Zhang Y, Ma P, et al. Ultrasensitive magnetic field-assisted surface plasmon resonance immunoassay for human cardiac troponin I. *Biosens Bioelectr*. 2017; 96: 288–293.
61. Nie W, Wang Q, Yang X, Zhang H, Zhiping Li, Lei Gao, et al. High sensitivity surface plasmon resonance biosensor for detection of microRNA based on gold nanoparticles-decorated molybdenum sulfide. *Anal Chim Acta*. 2017; 993: 55-62.
62. Wang Q, Li Q, Yang X, Wang K, Du S, Zhang H, et al. Graphene oxide-gold nanoparticles hybrids-based surface plasmon resonance for sensitive detection of microRNA. *Biosens Bioelectron*. 2016; 77: 1001–1007.
63. Li J, Lei P, Ding S, Zhang Y, Yang J, Cheng Q, et al. An enzyme-free surface plasmon resonance biosensor for real-time detecting microRNA based on allosteric effect of mismatched catalytic hairpin assembly. *Biosens Bioelectron*. 2016; 77: 435–441.
64. Yuan C, Lou Z, Wang W, Yang L, Li Y. Synthesis of Fe₃C@C from Pyrolysis of Fe₃O₄-Lignin Clusters and Its Application for Quick and Sensitive Detection of PrPSc through a Sandwich SPR Detection Assay. *Int J Mol Sci*. 2019; 20: 741.
65. Hong L, Lu M, Dinel MP, Blain P, Pengc W, Gu H, et al. Hybridization conditions of oligonucleotide-capped gold nanoparticles for SPR sensing of microRNA. *Biosens Bioelectron*. 2018; 109: 230–236.
66. Chen F, Wu Q, Song D, Wang X, Ma P, Sun Y. Fe₃O₄@PDA immune probe-based signal amplification in surface plasmon resonance (SPR) biosensing of human cardiac troponin I. *Coll Surf B Biointerfaces*. 2019; 177: 105-111.
67. Matuszczak E, Weremijewicz A, Komorowska M, Sankiewicz A, Markowska D, Debek W, et al. Immunoproteasom in the Plasma Patients with Moderate and Major Burns and Its Correlation with Proteasom and UCHL1 by SPR Imaging Biosensors. *J Burn Care Res*. 2018; 39: 948-953.
68. Lujambio A, Lowe SW. The microcosmos of cancer. *Nature*. 2012; 482: 347–355.
69. Zhu L, Wang K, Cui J, Liu H, Bu X, Ma H, et al. Label-Free Quantitative Detection of Tumor-Derived Exosomes through Surface Plasmon Resonance Imaging. *Anal Chem*. 2014; 86: 8857–8864.
70. Park J, Im H, Hong S, Castro CM, Weissleder R, Lee H. Analyses of intravesicular exosomal proteins using a nano-plasmonic system. *ACS Photonics*. 2018; 5: 487–494.
71. Ibn Sina AA, Vaidyanathan R, Dey S, Carrascosa LG, Shiddiky MJA, Trau M. Real time and label free profiling of clinically relevant exosomes. *Scient Rep*. 2016; 6: 30460.
72. Reiner AT, Ferrer NG, Venugopalan P, Lai RC, Lim SK, Dostálek J. Magnetic nanoparticle-enhanced surface plasmon resonance biosensor for extracellular vesicle analysis. *Analyst*. 2017; 142: 3913-3921.
73. Hosseinkhani B, van den Akker N, D'Haen J, Gagliardi M, Struys T, Lambrechts I, et al. Direct detection of nano-scale extracellular vesicles derived from inflammation-triggered endothelial cells using surface plasmon resonance. *Nanomedicine: Nanotechn. Biol. Medicine*. 2017; 13: 1663–1671.
74. Jia S, Li P, Koh K, Chen H. A cytosensor based on NiO nanoparticle-enhanced surface plasmon resonance for detection of the breast cancer cell line MCF-7. *Microchim Acta*. 2016; 183: 683–688.
75. Lamberti I, Scarano S, Esposito CL, Antoccia A, Antonini G, Tanzarella C, et al. *In vitro* selection of RNA aptamers against CA125 tumor marker in ovarian cancer and its study by optical biosensing. *Methods*. 2016; 97: 58–68.
76. David D, Surendran A, Thulaseedharan JV, Nair AS. Regulation of CNKSR2 protein stability by the HECT E3 ubiquitin ligase Smurf2, and its role in breast cancer progression. *BMC Cancer*. 2018; 18: 284.
77. Zhang T, Zheng Y, Zhao D, Yan J, Sun C, Zhou Y, et al. Multiple approaches to assess pectin binding to galectin-3. *Intern J Biol Macromolec*. 2016; 91: 994–1001.
78. Fernández MM, Ferragut F, Cárdenas Delgado VM, Bracalente C, Bravo AI, Cagnoni AJ, et al. Glycosylation-dependent binding of galectin-8 to activated leukocyte cell adhesion molecule (ALCAM/CD166) promotes its surface segregation on breast cancer cells. *Biochim Biophys Acta*. 2016; 1860: 2255–2268.
79. Han Y, Gao Y, He T, Wang D, Guo N, Zhang X, et al. PD-1/PD-L1 inhibitor screening of caffeoylquinic acid compounds using surface plasmon resonance spectroscopy. *Anal Biochem*. 2018; 547: 52–56.
80. Damborsky P, Zamorova M, Katrlík J. Determining the binding affinities of prostate-specific antigen to lectins: SPR and microarray approaches. *Proteomics*. 2016; 16: 3096–3104.
81. Ma L, Gu K, Zhang CH, Chen XT, Jiang Y, Melcher K, et al. Generation and characterization of a human nanobody against VEGFR-2. *Acta Pharmacol Sinica*. 2016; 37: 857–864.
82. Schlör A, Holzlöhner P, Listek M, Grief C, Butze M, Micheel B, et al. Generation and validation of murine monoclonal and camelid recombinant single domain antibodies specific for human pancreatic glycoprotein 2. *New Biotechnol*. 2018; 45: 60–68.
83. Lisi S, Fiore E, Scarano S, Pascale E, Boehman Y, Duconge F, et al. Non-SELEX isolation of DNA aptamers for the homogeneous-phase fluorescence anisotropy sensing of tau Proteins. *Anal Chim Acta*. 2018; 1038: 173-181.
84. Salehabadi H, Khajeh K, Dabirmanesh B, Biglar M, Amanlou M. Evaluation of angiotensin converting enzyme inhibitors by SPR biosensor and theoretical studies. *Enzyme Microb Technol*. 2019; 120: 117-123.
85. Gombau J, Nadal P, Canela N, Gómez-Alonso S, García-Romero E, Smith P, et al. Measurement of the interaction between mucin and oenological tannins by Surface Plasmon Resonance (SPR); relationship with astringency. *Food Chem*. 2019; 275: 397-406.
86. Singh P. Surface plasmon resonance (SPR) based binding studies of refolded single chain antibody fragments. *Biochemistry and Biophysics Reports*. 2018; 14: 83-88.